

Is there solid-on-solid contact in a sphere-wall collision in a viscous fluid?

Sumit Kumar Birwa, G. Rajalakshmi, Rama Govindarajan, and Narayanan Menon
TIFR Centre for Interdisciplinary Sciences, 21 Brundavan Colony, Narsingi, Hyderabad, India 500075 and
Department of Physics, University of Massachusetts, Amherst MA 01002, USA
 (Dated: November 11, 2016)

We study experimentally the process of normal collision between a sphere falling through a viscous fluid, and a solid plate below. As has previously been discovered, there is a well-defined threshold Stokes number above which the sphere rebounds from such a collision. Our experiment tests for direct contact between the colliding bodies, and contrary to prior expectations shows that solid-on-solid contact occurs even for Stokes numbers just above the threshold for rebounding. The details of the contact mechanics depend on the surface quality of the solids, but our experiments and a model calculation indicate that such contact is generic and will occur for any realistic surface roughness.

Collisions of solid particles in viscous fluids are relevant to many phenomena such as sedimentation, filtration, suspension flows, smoke and fog formation by aerosols. In addition to the complexities of hydrodynamic interactions between particles, to model these multiphase flows correctly, we also need an understanding of the mechanics of the collisions of particles with each other and with walls. In this article, we consider the simple situation of a ball falling towards a plane in a viscous fluid. From everyday experience, we know that a rubber ball will bounce after colliding with the floor. However, if the air is replaced with a highly viscous fluid the sphere can come to rest without bouncing. Our goal here is to determine whether solid-on-solid impact occurs during bouncing collisions, and more generally whether solid dissipation plays a role in determining the transition from bouncing to settling.

The collision between two smooth spheres was considered by Davis et al. [1] in 1986 within an elastohydrodynamic calculation. Working within the lubrication approximation, they suggested that the pressure in the thin fluid film between the spheres is large enough to produce an elastic deformation of the spheres. The stored elastic strain energy that is released in the form of kinetic energy was predicted to lead to rebound of the colliding particles without solid-on-solid contact. This idea is surprising as it suggests that a solid elastic sphere gets deformed by the fluid pressure sufficiently to reverse its momentum.

It is now generally held that the pertinent number that decides the dynamics of the bounce is the particle's Stokes number St , defined as

$$St = \frac{1}{9} \frac{\rho_s U D}{\mu} = \frac{1}{9} \frac{\rho_s}{\rho_f} Re \quad (1)$$

where U is the velocity of the sphere, D is the diameter of the sphere, ρ_s is the density of the sphere, ρ_f is the density of the fluid, μ is the dynamic viscosity of the fluid and Re is the Reynolds number of the sphere. The theory predicts a critical Stokes number St_c , below which the mutual approach between smooth bodies does not result in a bounce.

Experiments on sphere-wall collisions [2–6] find that the Stokes number does indeed collapse bouncing dynamics, and that there is a transition from bouncing to

settling at St ranging from about 8 to 15. (The velocity U changes with time during the collision, so the nominal value of St quoted is always estimated using the sphere velocity in the absence of wall effects). These experiments measure by video the coefficient of restitution, which is the ratio of the velocity just after the impact to the velocity just before the impact. Thus, zero coefficient of restitution signifies that there was no bounce. There is only a modest variation of the measured St_c with material [3, 5] e.g. Gondret et al. found similar St_c for teflon (Young's modulus, $Y = 0.5 GPa$) and tungsten carbide ($Y = 534 GPa$).

Surface roughness can begin to play a role when the fluid layer separating the solids becomes comparable to the height of the asperities. Davis [6, 7] included the effect of surface roughness by solving the equation of motion in two steps, first using the lubrication approximation until a cutoff distance set by the roughness, and then reversing the motion using the dry coefficient of restitution for an inelastic collision. Barnocky and Davis [6] experimentally explored the predicted logarithmic dependence of St_c on the surface roughness. Joseph et al. [4] use spheres with well-characterized roughness and argued that the differing level of scatter in their data from one type of sphere to another can be explained by surface roughness. Other short-range forces such as Van Der Waals forces could conceivably play a role very close to contact, but these are not considered in these pictures of bouncing.

However, whether contact occurs or not during rebound is still not established. All the experiments till now have been conducted using high speed cameras which cannot resolve spatially or temporally the contact dynamics. It is essential to study the dynamics close to the impact point, both in time and space to clearly check when and how contact occurs. However, it is reasonable to believe that smooth bodies can come in contact during rebound at large Stokes numbers. In the current experiment we directly address the existence and influence of solid-on-solid contact using an electrical set-up to investigate the kinetics very close in time to the moment of impact.

In our experiments, stainless steel spheres were dropped on a stainless steel plate of 10cm x 10cm x

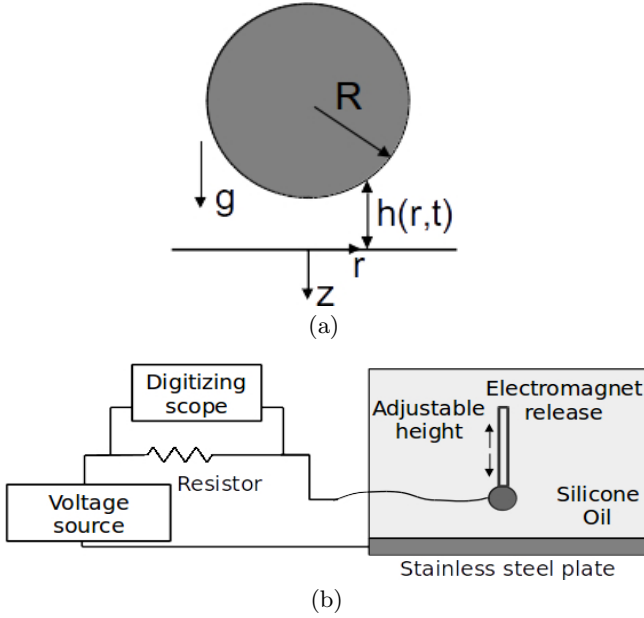


FIG. 1. (a) A sphere approaching a plane, where r, z are the radial and vertical directions, $D = 2R$ is the diameter of the sphere, g is the acceleration due to gravity, and $h(r, t)$ is the time-dependent distance between sphere and the bottom wall. (b) Schematic diagram of experimental set-up.

1cm thickness through silicone oil of dynamic viscosity $\mu = 346 \pm 20 \text{ cP}$, and density $\rho_f = 970 \text{ kg/m}^3$. As shown in Figure 1(a), a voltage was applied between the plate surface and the sphere and the current through the resistor was observed on a digital oscilloscope (Tektronics DPO 4054B) at a sampling rate of 1 to 5 MHz. When the sphere makes or breaks metallic electrical contact with the plate, the circuit closes or opens [8]. Both direct current (dc) and alternating current (ac) voltage sources were used in the experiments.

The spheres were released by an electromagnet Figure 1(b) from different initial heights using a micrometer translation stage allowing us to control the incoming velocity and the Stokes number. The release height ranged from 1mm to 70mm, and was determined to an accuracy of $20 \mu\text{m}$ approximately, which resulted in a maximum error of 2% at the lowest height. For each release height, the nominal Stokes number at impact was determined from the velocity computed at the position of the plate's surface in the absence of the plate. To obtain this velocity, we solved the equation of motion of the ball under gravity, buoyancy and viscous drag for which we used an empirical formula [9] applicable to our experimental range of Reynolds number which varies from $Re = 5.7$ to 32,

$$(\rho_s - \rho_f)Vg - 6\pi\mu RU(1 + 0.15Re^{0.687}) = \rho_s V \frac{\partial U}{\partial t} \quad (2)$$

where V is the volume of the sphere. The resulting Stokes number ranged from 5 to 28 with a maximum error of

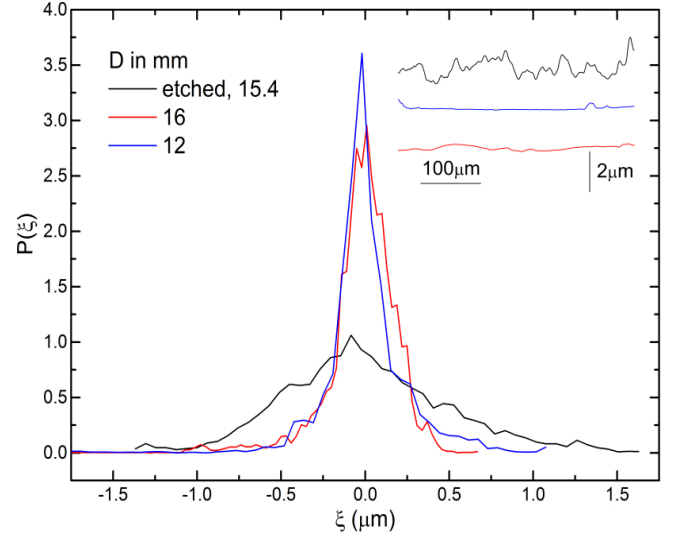


FIG. 2. Probability density $P(\xi)$ of roughness of spheres as measured with a contact profilometer. To obtain the roughness ξ , the path traced by profilometer as a function of distance has been subtracted from the gross curvature of the sphere. The inset shows typical profiles $\xi(s)$ of roughness as a function of the position s along the surface, for all the three spheres used.

6.5% at the largest Stokes number (including contributions from temperature dependence of viscosity and precision of release height).

We used two types of spheres in the experiments. One was as-purchased stainless steel ball bearings with density $\rho_s = 7630 \text{ kg/m}^3$ in two diameters, $D = 16 \text{ mm}$ and 12 mm . The second type of sphere, $D = 15.4 \text{ mm}$, was produced by etching the $D = 16 \text{ mm}$ balls with HNO_3 in a 1:3 aqueous solution for 10 minutes. We measured their surface topography with a Dektak contact profilometer and extracted the position-dependent roughness from the difference ξ between the measured height, and the best-fit spherical profile. The as-purchased spheres had smooth patches of small rms roughness around $\sim 0.025 \mu\text{m}$ interspersed by very widely separated pits (of typical height $1 - 2 \mu\text{m}$) and mounds (of typical height $0.25 \mu\text{m}$), with lateral size $\sim 10 \mu\text{m}$. These numbers varied slightly from sphere to sphere. The etched spheres had larger, but more uniform roughness with an rms value $\sim 0.4 \mu\text{m}$ but several larger peaks of the order of $1 - 2 \mu\text{m}$. The typical lateral scale of the roughness is $\sim 100 \mu\text{m}$. Histograms of the roughness are shown in Figure 2 with examples of the roughness $\xi(s)$ as a function of coordinate on the sphere surface (s) [10].

In Figure 3 we show examples of the regimes of behaviour observed in our experiments with data obtained both by applying AC (Figure 3 a, c, d) and DC voltages (Figure 3 b) between plate and sphere. At very low Stokes number (panel(a) $St = 5.8$), we observe no bounces. The first electrical contact persists for all time but can be noisy, presumably due to rolling or rocking

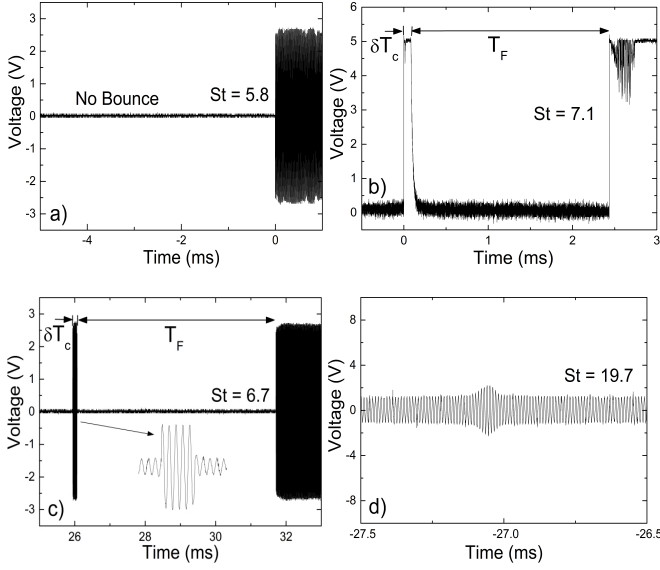


FIG. 3. Voltage vs time graphs for $D = 16\text{mm}$ sphere showing bounce and No bounce cases for DC and AC runs. (a) No bounce observed at Stokes number = 5.8 for AC case, (b) Bounce observed for DC run at Stokes number = 7.1, (c) Bounce observed for AC run at Stokes number = 6.7, (d) Bounce without contact (notice the small rise in voltage) shown for AC run at $St = 19.7$.

of the sphere. At larger values of the Stokes number, as shown in Figure 3 (b) and (c), the ball makes metallic contact for a finite contact time, δT_c . It then breaks contact and is in the fluid for a flight time T_F before settling to a permanent electrical contact. There is a clear separation of scale between the contact time, δT_c (tens of $\mu\text{-sec}$) and the flight time, T_F (tens of milli-sec). Finally, we see occasional instances, as shown in Figure 3d, of capacitive contact between the ball and the plate.

In order to test that electrical forces do not play a role in the mechanics of the contact, we have compared our results with high frequency AC (100 to 500kHz) to results with a DC voltage, and have made measurements as a function of the amplitude of the applied voltage. In all cases, the data appear to be unaffected by the electrical voltage [10]. We have also chosen silicone oil as it has a high dielectric breakdown voltage ($> 400\text{kV/cm}$).

The major qualitative result in Figure 3 is that there is direct mechanical contact between the ball and the plate during the bounce, in contrast to expectations based on elastohydrodynamic theories [1]. Next, we explore the regime and nature of that contact.

We define contact fraction, ϕ , as the fraction of experiments at a particular Stokes number in which the sphere made contact with the plate's surface during the bounce i.e. collisions as shown in Figure 3 (b) and (c). In Figure 4 (a), we plot the contact fraction, ϕ , as a function of Stokes number. The value of ϕ rises sharply from zero above a critical Stokes number $St > St_c$, which is the

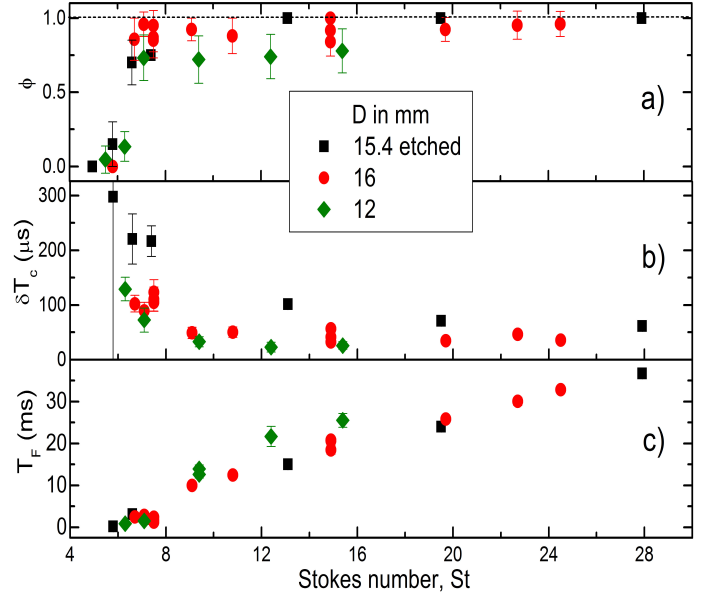


FIG. 4. Contact fraction (ϕ), Contact time (δT_c), and Flight time (T_F) vs Stokes number for 15.4mm etched ball, 16mm and 12mm unetched-balls.

same for all three types of spheres we used. The value of $St_c \approx 6.2 \pm 0.5$ that marks the transition to bouncing with mechanical contact is consistent with the bouncing transition within the scatter of previous experiments [2–4]. Thus solid-on-solid contact occurs even just above the threshold of bouncing.

In Figure 4 (b) we show data for the duration of contact, δT_c . The contact time δT_c decreases slowly as the Stokes number is increased above St_c . Calculations for a Hertzian, elastic impact [11] predict a very weak dependency of contact time on velocity, $\delta T_c \propto (UR_{eff})^{-1/5}$, where R_{eff} is the effective radius at the point of contact. For perfectly smooth spheres, $R_{eff} = R$, whereas the R_{eff} will be smaller when a bump on the sphere is presented to the plane. Contact times for the etched spheres are slightly longer than those for the unetched spheres (which have very similar contact times for both sizes of sphere). The roughness of the sphere, rather than the sphere radius, possibly sets the relevant curvature at impact and therefore influences the contact time. (We discuss the relative scales of roughness and Hertzian impact size in the Supplementary Information).

In Figure 4 (c) we show data for the time spent in between the bounce and the next collision, which we refer to as the flight time T_F . This is a measure of the kinetic energy with which the ball rebounds from the plate. As expected, this is an increasing function of $(St - St_c)$. Furthermore, there is little or no variation with the type of sphere used, as opposed to the data for δT_c . This implies that the details of the solid contact may not affect the total dissipation, as elaborated below.

Thus far, we have discussed mean values of the contact

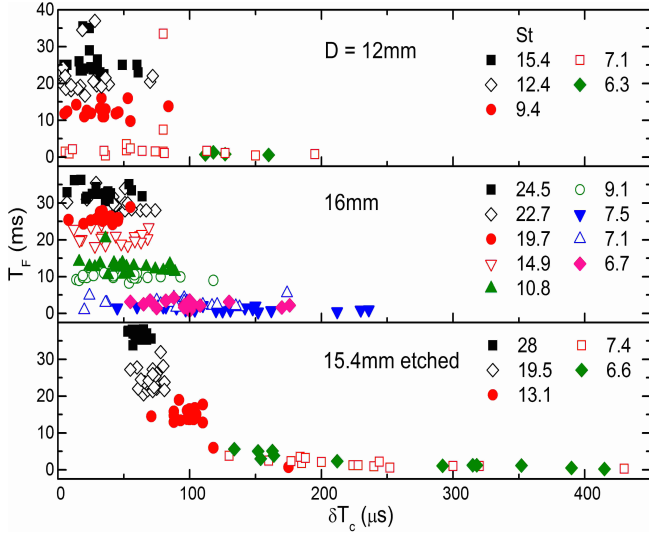


FIG. 5. Contact time vs Flight time for 16mm un-etched ball, 12 mm ball and 16mm etched ball, respectively. Notice the increase in scatter percentage at lower Stokes number.

duration and flight times, averaged over experimental trials for a fixed St . However, studying the distribution of δT_c and T_F is revealing of the source of the dissipation and its relationship to surface roughness. In Fig. 5 we plot T_F versus δT_c for the two unetched spheres and the etched sphere for Stokes numbers varying from just above St_c to about $St = 28$. In most cases, we find a very broad distribution of contact times at a fixed value of St , varying by up to an order of magnitude. Presumably this reflects the variation in the local topography of the sphere. At the same time, we find much smaller variability in the flight time, particularly at larger Stokes number. Thus the total dissipation that occurs in the sphere-wall encounter, as reflected by the flight time, is not strongly affected by the duration of solid-on-solid contact. That is, the results indicate that despite the solid contact, the bulk of the kinetic energy of the sphere is lost to fluid dissipation in the collision.

At the largest Stokes number a different trend sets in, most clearly observed in the etched spheres: the contact time T_c , also becomes well-defined. We suggest that this reflects the fact that at large impact speeds, the effective radius of the Hertzian contact becomes substantial, and averages over the roughness of the etched sphere. Thus collisions at different locations are effectively similar in their contact mechanics and no longer depend on the details of the roughness. We might imagine yet another regime – as in the example of a ball bouncing in air – at even higher Stokes numbers where the dissipation becomes solid-dominated, but we do not explore that regime in our experiments. Indeed, even at the larger Stokes numbers we explore in this experiment, we begin to observe plastic deformation in the form of pitting at the point of impact.

While the data make a clear case for solid-on-solid contact in all the spheres used, the St -dependence of the details of the bounce appear to be influenced by the surface quality of the sphere. This may lead one to question whether our observations are relevant for spheres that are even smoother than the ball bearings employed in this study. A calculation for a rigid, smooth, sphere within the lubrication approximation is illuminating in this regard. As shown below, roughness on the nanometre scale is sufficient to generate a solid collision.

Following [1] we write the equation of motion for a smooth sphere approaching a plane within the lubrication approximation. The vertical distance between ball and plane varies according to

$$\rho_s V \ddot{h}_o = (\rho_s - \rho_f) V g - 6\pi\mu R \dot{h}_o (1 + 0.15 Re^{0.687}) - F_p \quad (3)$$

where $h_o = h(0, t)$ and Re is defined by the instantaneous velocity of the sphere, \dot{h}_o (see Figure 1 (a)). We have neglected added-mass effects in the acceleration, and as in Equation (2), we use an empirical formula for the viscous drag in the absence of a bottom plate. The upward pressure force exerted by the fluid layer is denoted F_p . Within the lubrication approximation the radial velocity of the fluid squeezing out between the plate and sphere has a parabolic profile. This leads to a horizontal force balance between pressure gradient and viscous forces:

$$\frac{\partial p}{\partial r} + \mu \frac{\partial^2 u_r}{\partial z^2} = 0, \quad (4)$$

where, $p(r, t)$ is the pressure. Integrating Equation 4 over the height profile of the sphere

$$h(r, t) = h_o(t) + R - \sqrt{R^2 - r^2}, \quad (5)$$

between $r = 0$ and $r = R$ gives the net pressure force F_p . Equation 3 is then numerically solved to obtain h_o as a function of time starting from a range of initial heights as in the experiment. Results for the velocity \dot{h}_o as a function of height h_o are shown for different Stokes numbers in Figure 6. Even within this approximate treatment, where p diverges as $h_o \rightarrow 0$, the velocity is significant and finite even for a roughness cut-off as small as $1nm$ for large enough St . Thus the indication from this calculation is that collision occurs even when the spheres are atomically smooth.

The lubrication approximation is questionable at small enough distances; to make further quantitative comparison with experiments will possibly require going beyond elastohydrodynamic lubrication theory by direct numerical simulation. However, it seems clear that direct solid contact is likely to be a general feature, even close to the threshold of bouncing. Within this regime, however, the dissipation remains dominated by fluid mechanics, and the contact mechanics are largely controlled by surface roughness and bulk solid properties. Even though solid dissipation does not play a prominent role, the presence of solid-to-solid contact is potentially of great significance

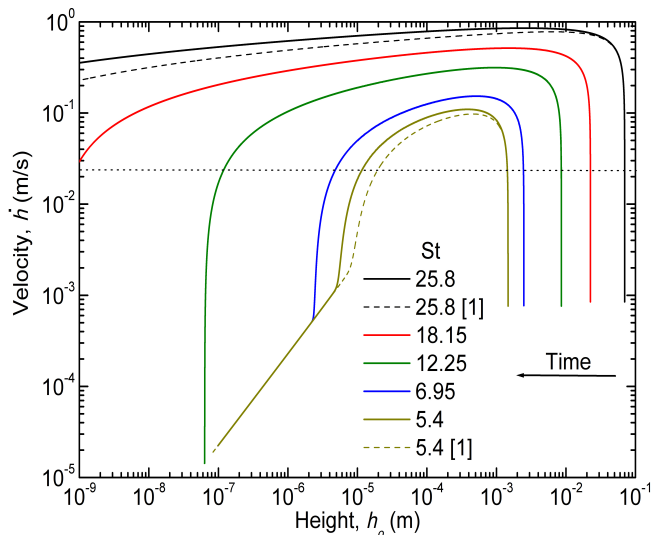


FIG. 6. Velocity of a rigid smooth sphere as it approaches a flat surface in a viscous medium under the equation of motion 3. The dimensional axes are based on a steel sphere of diameter 16mm, dropped from different heights. The horizontal line at a velocity of 0.021m/s is the critical velocity at height 1nm and 10nm required to move the sphere up by the same height (1nm or 10nm) when the direction of the velocity is reversed.

in several contexts such as wear, charge transfer, or chemical reactivity of solids in suspension.

We acknowledge funding from TCIS Hyderabad, the APS-IUSSTF for a travel grant to SKB, and NSF-DMR 120778 and nsf-dmr 1506750 for support at UMass Amherst. We are grateful for the use of the Nanotechnology facility for roughness measurements.

-
- [1] R. H. Davis, J.-M. Serayssol, and E. Hinch, *Journal of Fluid Mechanics* 163, 479 (1986).
 - [2] P. Gondret, E. Hallouin, M. Lance, and L. Petit, *Physics of Fluids* 11, 2803 (1999).
 - [3] P. Gondret, M. Lance, and L. Petit, *Physics of Fluids* 14, 643 (2002).
 - [4] G. Joseph, R. Zenit, M. Hunt, and A. Rosenwinkel, *Journal of Fluid Mechanics* 433, 329 (2001).
 - [5] R. Zenit and M. L. Hunt, *Journal of Fluids Engineering* 121, 179 (1999).
 - [6] G. Barnocky and R. H. Davis, *Physics of Fluids* 31, 1324 (1988).
 - [7] R. H. Davis, *PhysicoChem. Hydrodyn* 9, 41 (1987).
 - [8] H. King, R. White, I. Maxwell, and N. Menon, *EPL (Europhysics Letters)* 93, 14002 (2011).
 - [9] R. C. Flagan and J. H. Seinfeld, *Fundamentals of Air Pollution Engineering* (Prentice-Hall, Inc., 1988).
 - [10] S. Birwa, G. Rajalakshmi, R. Govindarajan, and N. Menon, See supplementary material for this paper.
 - [11] L. D. Landau and E. Lifshitz, *Theory of Elasticity*, vol. 7, Vol. 3 (Elsevier New York, 1986) p. 109

Supplementary Information: Is there solid-on-solid contact in a sphere-wall collision in a viscous fluid?

I. EFFECT OF ELECTRICAL FORCES

We carried out collision experiments to measure contact times and contact fractions as a function of the amplitude of the applied AC or DC voltages, and of the frequency of the applied voltage. In Figure S1 we show data for a fixed Stokes number ($St = 19.7$) and diameter = 16mm. The applied AC voltage and frequency were varied from 2V to 5.3V and from 100 KHz to 500 KHz. The DC voltage was varied from 1.5V to 5V. As is evident in the figure S1, no systematic dependence of contact time on supply voltage was observed. This suggests that electrical forces do not play a role in the dynamics of the collision. In particular, there is no observed change in the nature of the electrical signal, arguing that dielectric breakdown of silicone oil does not occur during the collision process. The literature value of the breakdown voltage is high but finite ($> 400kV/cm$), so perhaps breakdown is avoided due to the very short time-scales of interaction. We thus infer that the values of contact time, flight time and contact fraction reported in this article are independent of voltage applied.

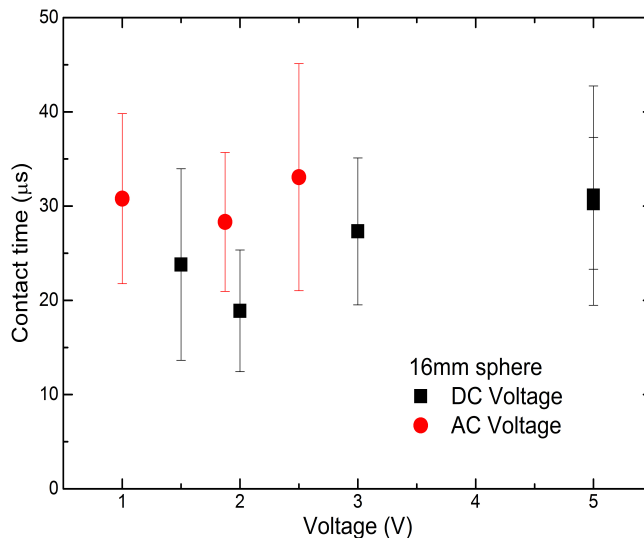


FIG. S1. Contact time averaged over 20 trials at different voltages (AC and DC) and different frequencies for 16mm sphere at 19.7 Stokes number. The contact time does not show a systematic trend with voltage.

II. ROUGHNESS

The roughness profile of spheres used was measured with a diamond-tip Dektak contact profilometer with lateral resolution of $0.5\mu m$ and vertical range of $65.5\mu m$. The vertical resolution of profilometer is $\approx 1nm$. The profilometer tip travels along a path of length $\sim 0.4mm$ along the surface of the sphere. We fit a circle to the height along the path traced by profilometer. This yields the global radius of curvature along this path as shown in FIG. S2. The deviations from this fit give the local roughness, ξ of the topography of the surfaces. As can be seen from the statistics of ξ given in Table S1, the etched 15.4mm sphere's surface was found to be most rough; as discussed in the main text, it is also the least heterogeneous, with relatively uniform roughness across the surface.

Table S1. Roughness values

	12mm	16mm	15.4mm
RMS (μm)	0.25	0.22	0.5
Max deviation (μm)	1.1	0.68	1.66
Min deviation (μm)	-1.78	-1.77	-1.4

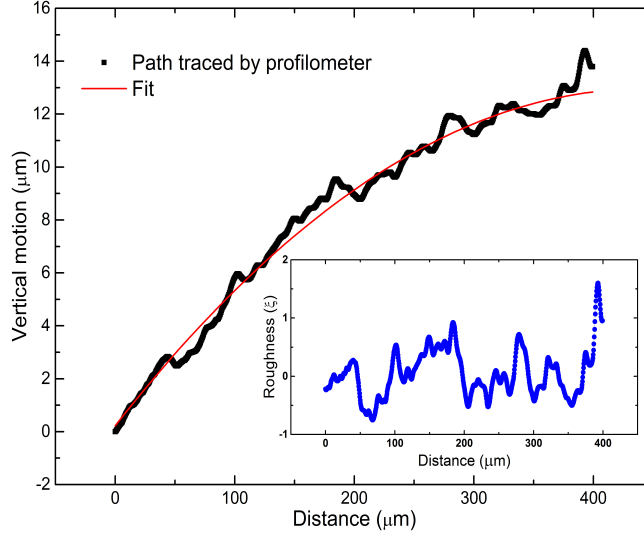


FIG. S2. A fit for the 15.4 mm etched sphere on the path traced by the profilometer as a function of position along a line on the sphere's surface is shown in red. The fit gives us the global curvature of the path and the local roughness of the sphere is obtained by subtracting the surface profile from this fit. The roughness (ξ) is shown in blue in the inset.

III. HERTZIAN CALCULATION

For a perfect normal collision between two smooth, perfectly elastic spheres of radii R_i , masses m_i , Young's modulus E_i , and Poisson ratio σ_i ($i=1,2$), the closest approach of the spheres during mechanical contact can be calculated by Hertzian theory [S1] and is given by

$$b = \left(\frac{m_{eff}}{k} \right)^{2/5} v^{4/5} \quad (S1)$$

where b is the maximum overlap of the spheres ($b =$ distance between the centres of the sphere - $(R_1 + R_2)$) and v is the relative velocity between the spheres just before contact. Here m_{eff} is the reduced mass of the spheres and is given by

$$\frac{1}{m_{eff}} = \frac{1}{m_1} + \frac{1}{m_2} \quad (S2)$$

k is the effective modulus of the spheres,

$$k = \frac{4}{5D_0} \sqrt{\frac{R_1 R_2}{R_1 + R_2}} \quad (S3)$$

D_0 is

$$D_0 = \frac{3}{4} \left(\frac{1 - \sigma_1^2}{E_1} + \frac{1 - \sigma_2^2}{E_2} \right). \quad (S4)$$

In our set-up, one of the sphere has been replaced by a plate, so $1/R_2 = 0$ and $1/m_2 = 0$.

For a smooth sphere of diameter 15.4 mm, the depth of the contact formed due to collision of the sphere with the plate for an impact velocity corresponding to $St = 28$ is $\approx 13.5 \mu m$. The radius of the contact area is then given by

$$a = \sqrt{2Rb} \quad (S5)$$

This gives the diameter of the contact area $= 2a \approx 900 \mu m$. Of course, due to lubrication forces, the actual impact velocity will be much lower, so these calculations considerably overpredict the size of the crater made.

A different possibility is that instead of the radius of the sphere setting the geometry of the collision, the local radius of curvature set by the roughness of the sphere is the relevant radius. If the characteristic height of bumps is q and the characteristic lateral size is l , the local radius of curvature will be given by

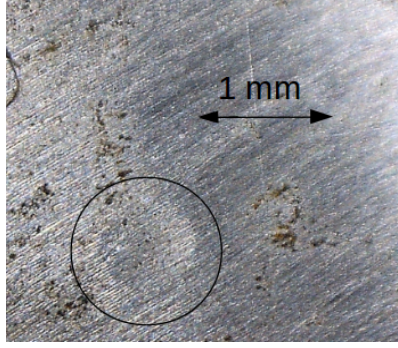


FIG. S3. Craters visible inside the marked circle. The sizes of the crater on the plate is around $700 \mu\text{m}$ for 28 Stokes number.

$$R_{local} = \frac{1}{2q} \left(\frac{l}{2} \right)^2 \quad (\text{S6})$$

For $q = 1 \mu\text{m}$ and $l = 100 \mu\text{m}$, $R_{local} = 900 \mu\text{m}$. If we use this radius in Hertzian calculation for collision, we get the depth and radius of the contact area to be $\approx 20 \mu\text{m}$ and $200 \mu\text{m}$, respectively.

At the largest Stokes numbers, we see that the sphere's impact on the plate leaves small craters (FIG. S3) $\approx 700 \mu\text{m}$, thus the Hertzian calculation must be replaced by a calculation involving material plasticity. Finally, we recall that all these estimates have used the Stokes number computed without wall effects (as discussed in main article), thus the actual impact velocity will be lower. These estimates therefore overpredict the size of the region of contact.

[S1] L. D. Landau and E. Lifshitz, Theory of Elasticity, vol. 7, Vol. 3 (Elsevier New York, 1986) p. 109.